

# Super-luminous supernovae: $^{56}\text{Ni}$ power versus magnetar radiation

Luc Dessart,<sup>1,2\*</sup> D. John Hillier,<sup>3</sup> Roni Waldman,<sup>4</sup> Eli Livne,<sup>4</sup> Stéphane Blondin<sup>5</sup>

<sup>1</sup>: *Laboratoire d'Astrophysique de Marseille, Université Aix-Marseille & CNRS, UMR 7326, 38 rue Frédéric Joliot-Curie, 13388 Marseille, France*

<sup>2</sup>: *TAPIR, Mail code 350-17, California Institute of Technology, Pasadena, CA 91125, USA*

<sup>3</sup>: *Department of Physics and Astronomy, University of Pittsburgh, USA*

<sup>4</sup>: *Racah Institute of Physics, The Hebrew University, Jerusalem, Israel*

<sup>5</sup>: *Centre de Physique des Particules de Marseille, Université Aix-Marseille, CNRS/IN2P3, 163 avenue de Luminy, 13288 Marseille, France*

Accepted 2012 August 05. Received 2012 July 02; in original form 2012 May 20

## ABSTRACT

Much uncertainty surrounds the origin of super-luminous supernovae (SNe). Motivated by the discovery of the Type Ic SN 2007bi, we study its proposed association with a pair-instability SN (PISN). We compute stellar-evolution models for primordial  $\sim 200 M_{\odot}$  stars, simulating the implosion/explosion due to the pair-production instability, and use them as inputs for detailed non-LTE time-dependent radiative-transfer simulations that include non-local energy deposition and non-thermal processes. We retrieve the basic morphology of PISN light curves from red-supergiant (RSG), blue-supergiant (BSG), and Wolf-Rayet (WR) star progenitors. Although we confirm that a progenitor  $100 M_{\odot}$  helium core (PISN model He100) fits well the SN 2007bi light curve, the low ratios of its kinetic energy and  $^{56}\text{Ni}$  mass to the ejecta mass, similar to standard core-collapse SNe, conspire to produce cool photospheres, red spectra subject to strong line blanketing, and narrow line profiles, all conflicting with SN 2007bi observations. He-core models of increasing  $^{56}\text{Ni}$ -to-ejecta mass ratio have bluer spectra, but still too red to match SN 2007bi, even for model He125 – the effect of  $^{56}\text{Ni}$  heating is offset by the associated increase in blanketing. In contrast, the delayed injection of energy by a magnetar represents a more attractive alternative to reproduce the blue, weakly-blanketed, and broad-lined spectra of super-luminous SNe. The extra heat source is free of blanketing and is not explicitly tied to the ejecta. Experimenting with a  $\sim 9 M_{\odot}$  WR-star progenitor, initially exploded to yield a  $\sim 1.6 B$  SN Ib/c ejecta but later influenced by tunable magnetar-like radiation, we produce a diversity of blue spectral morphologies reminiscent of SN 2007bi, the peculiar Type Ib SN 2005bf, and super-luminous SN 2005ap-like events.

**Key words:** stars: magnetars – stars: atmospheres – stars: supernovae

## 1 INTRODUCTION

In the last decade, a number of super-luminous supernovae (SNe) have been identified but their origin remains highly uncertain. Most of these exhibit the Type Ia/Ib/Ic SN light-curve morphology, merely “expanded” to form a broader and brighter peak. In this category, we find a zoo of events including, e.g., the Type IIn SN 2006gy (Smith et al. 2007), the peculiar type Ib SN 2005bf (Folatelli et al. 2006; Maeda et al. 2007) with its double-peak light curve, the type Ic SN 2007bi (Gal-Yam et al. 2009) with its extended nebular tail, the linearly-declining SN 2008es (Gezari et al. 2009), as well as a rather uniform group of SNe at redshifts of 0.2–1.2 with a unique, nearly-featureless, blue continuum, and a fast fading nebular flux (Quimby et al. 2011). Today, three mechanisms are proposed for these super-luminous events, representing extreme versions of SNe interacting with a circumstellar medium,

$^{56}\text{Ni}$ -powered SNe, and magnetar-powered SNe. For brevity, and since an interaction mechanism is believed not to be relevant to SN 2007bi, we restrict our discussion to the last two mechanisms.

Historically, the most natural way to explain a large SN luminosity is the production of a larger-than-average  $^{56}\text{Ni}$  mass (Colgate & McKee 1969). The essential feature is that because the half-life of  $^{56}\text{Ni}$  is 6.075 d and that of its daughter nucleus  $^{56}\text{Co}$  is 77.23 d, radioactive-decay energy can reheat the ejecta once it has expanded to  $\gtrsim 10^{14}$  cm and become less sensitive to  $PdV$  losses. However, “standard” core-collapse SNe are generally ineffective  $^{56}\text{Ni}$  producers – the  $^{56}\text{Ni}$  production is strongly conditioned and limited by the explosion energy and the progenitor structure. Today, highly energetic magneto-rotational explosions are expected to be the most suitable means to produce super-luminous SNe (Burrows et al. 2007). These are generally nicknamed “hypernovae”, and are distinct from the more germane neutrino-driven core-collapse SN explosions (Buras et al. 2006).

Pair-instability SNe (PISNe) represent an alternative for pro-

\* email: Luc.Dessart@oamp.fr

ducing a large amount of  $^{56}\text{Ni}$ . In the exceptional instance of stars with a main-sequence mass in the range  $140\text{--}260 M_{\odot}$ , expected to form at low metallicity in the early Universe (Bromm & Larson 2004),  $e^{-}e^{+}$  pair production may lead to an explosion and give rise to a PISN (Barkat et al. 1967; Heger & Woosley 2002; Langer et al. 2007; Waldman 2008). Although the explosion mechanism is robust, it is still unclear whether such massive stars can form. If they do form, their mass loss is of concern as it can considerably affect the final stellar mass and radius, and thus, the resulting explosion properties, SN radiation, and detectability (Scannapieco et al. 2005; Kasen et al. 2011).

An alternative means to produce a bright display is by magnetar radiation (Wheeler et al. 2000; Maeda et al. 2007; Kasen & Bildsten 2010; Woosley 2010). The energy lost in the process leads to the spin down of the magnetar, which eventually quenches its power. For a dipole field, the spin-down time scale is  $t_{\text{sp}} \sim 4.8 B_{15}^{-2} P_{10}^2 \text{ d}$ , where  $B_{15}$  is the magnetic-field strength in  $10^{15} \text{ G}$  and  $P_{10}$  the rotation period  $P$  in units of 10 ms. For suitable choices of  $B_{15}$  and  $P_{10}$ , this timescale can be comparable to the half-life of  $^{56}\text{Ni}/^{56}\text{Co}$  and consequently makes magnetar radiation an attractive substitute for long-lived super-luminous SNe - in combination with different ejecta masses, it also provides a natural modulation for the time to peak brightness, the luminosity at peak (Kasen & Bildsten 2010), as well as for the fading rate from peak.

The proposition that SN 2007bi is a PISN is controversial. It was discovered around the peak of the light curve ( $M_R \sim -21 \text{ mag}$ ), revealed a slowly fading  $R$ -band magnitude consistent with full  $\gamma$ -ray trapping from  $\sim 5 M_{\odot}$  of  $^{56}\text{Ni}$  (Fig. 1). It exploded in an environment with a metallicity of one third solar, which conflicts with star formation (Bromm & Larson 2004) and evolution theory (Langer et al. 2007), which expect such stars to form and explode as a Type Ic SN at much lower metallicity only. Gal-Yam et al. (2009) performed a few simulations for SN 2007bi, covering a range of progenitor He cores and thus explosion characteristics, and found their He100 model to be adequate. From their modeling of a nebular-phase spectrum, they infer ejecta masses compatible with the PISN scenario. Improving upon the original work of Scannapieco et al. (2005), Kasen et al. (2011) studied a broad mass range of PISN progenitor models including RSG, BSG, and WR stars. Their He100 model gives a suitable match to the SN 2007bi light curve, as well as a rough agreement with the near-peak spectrum.

An alternative scenario, involving the collapse of a massive-star core, has been proposed by Moriya et al. (2010). In association with the extreme properties of the SN explosion they also invoke radioactive-decay energy to explain the light curve. The situation remains blurred, epitomized by the rough compatibility of both the  $^{56}\text{Ni}$  model (PISN model He100 or extreme core-collapse SN) and the magnetar model for explaining the SN 2007bi light curve (Kasen & Bildsten 2010; Kasen et al. 2011). Understanding what distinguishes these different scenarios is thus critical to identify the nature of super-luminous SNe.

In the next section we present the numerical setup for the in-depth study of PISN explosions that we have undertaken, and which will be discussed more fully elsewhere (Dessart et al., in prep). Simulation results for three different PISN progenitor models are presented in Sect. 3. We then focus on the model He100 that was proposed for SN 2007bi, and discuss its incompatibilities with the observations. Ways of alleviating these incompatibilities are discussed in Sect. 4. In particular we propose two means to produce a super-luminous SN with a bluer color – either through an increase

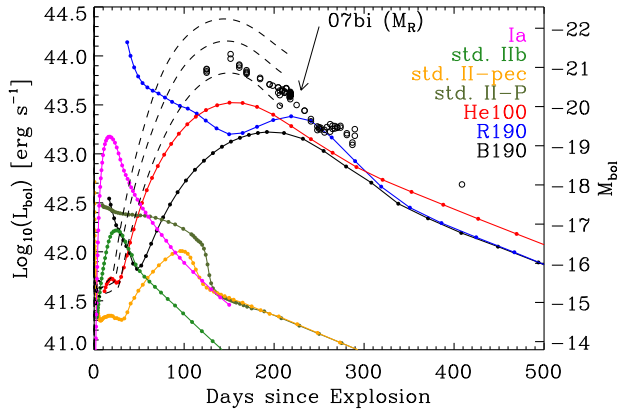


**Figure 1.** Synthetic bolometric light curves extracted from our CMFGEN simulations of PISNe and other “standard” SN models (solid). We include v1D light curves for models He105, He115, and He125 of increasing peak luminosity (dashed) and the estimated SN 2007bi absolute  $R$ -band magnitude (Gal-Yam et al. 2009, circles).

in the  $^{56}\text{Ni}$ -mass to ejecta mass ratio or, alternatively, through a delayed energy injection from the compact remnant (Sect. 4).

## 2 NUMERICAL SETUP OF PISN SIMULATIONS

The work presented in this paper was produced in several independent steps. First, a large grid of massive-star progenitors with main-sequence masses in the range  $160\text{--}230 M_{\odot}$  were evolved with MESA (Paxton et al. 2011) until central  $^{20}\text{Ne}$  exhaustion, assuming  $10^{-4} Z_{\odot}$  and no rotation. At that time, these stars are either RSG, BSG, or WR stars. These simulations are then remapped onto the 1D radiation-hydrodynamical code v1D (Livne 1993), with allowance for (explosive) nuclear burning and radiation transport. At  $^{20}\text{Ne}$  exhaustion, oxygen is naturally ignited and consumed in less than a minute to  $^{56}\text{Ni}$  and intermediate-mass elements (IMEs). We model this explosion phase and the later evolution of the ejecta for a few years (Waldman et al., in prep.).

Here, we focus on three PISN types: 1) II-P: Model R190 from a  $190 M_{\odot}$  main-sequence star and dying as a  $164.1 M_{\odot}$  RSG with a surface radius of  $4044 R_{\odot}$ ; 2) II-pec: Model B190 from a  $190 M_{\odot}$  main-sequence star and dying as a  $133.9 M_{\odot}$  BSG with a surface radius of  $186.1 R_{\odot}$ ; 3) Ic (or Ib): Model He100 from a  $100 M_{\odot}$  helium core ( $190 M_{\odot}$  initially, artificially stripped of its hydrogen envelope, but without subsequent mass loss) and dying as a  $100 M_{\odot}$  WR with a surface radius of  $1.2 R_{\odot}$ . In the same order, these models synthesize  $2.63$ ,  $2.99$ , and  $5.02 M_{\odot}$  of  $^{56}\text{Ni}$ , have kinetic energies of  $33.2$ ,  $34.5$ , and  $37.6 \text{ B}$ , and a representative expansion velocity  $v_{\text{rep}} \equiv \sqrt{2E/M} \sim 5000 \text{ km s}^{-1}$ .

Although PISNe are thermonuclear explosions, akin to SNe Ia, burning only occurs in the inner ejecta so that  $^{56}\text{Ni}$  is ultimately confined to shells moving with velocities inferior to  $2000 \text{ km s}^{-1}$  (models R190 and B190) and  $4000 \text{ km s}^{-1}$  (He100). In the second part of this letter, we present additional He models, similar to He100, but with initial masses from  $105$  to  $125 M_{\odot}$ , spaced every  $5 M_{\odot}$  (Sect. 4). The properties of our hydrodynamical input models are comparable to those of Kasen et al. (2011), so we defer their detailed presentation to Waldman et al. (in prep.).

For the radiative-transfer calculations of light curves and spectra, we adopt our standard procedure (Dessart & Hillier 2010,

2011; Dessart et al. 2011, 2012). Hillier & Dessart (2012) have recently given a full description of the code CMFGEN for SN calculations. We perform time-dependent simulations for the full ejecta, from the photospheric to the nebular phase. We start when homologous expansion is reached (a few days to a few weeks after explosion) and use as initial conditions the ejecta chemical stratification and structure computed with V1D. Our radiative-transfer simulations are fully time-dependent, non-LTE, include non-local energy deposition, treat non-thermal processes associated with  $\gamma$ -rays, and yield synthetic spectra from the far-UV to the far-IR. We treat explicitly the effects of line blanketing arising from the presence of a multitude of optically-thick lines of metals. Expansion strengthens line blanketing by broadening the effective width of lines, increasing the occurrence of line overlap (Hillier & Miller 1998).

### 3 RESULTS AND COMPARISON TO SN 2007bi

The synthetic light curves computed for PISN models R190, B190, and He100 reflect their large ejecta and  $^{56}\text{Ni}$  masses, and are characterized by a high-brightness phase that lasts a few hundred days. Their peak luminosities are on the order of  $10^{10} L_{\odot}$ . They transition to the nebular phase, with a luminosity reflecting the rate of  $^{56}\text{Co}$  decay-energy release,  $\sim 200$  d after peak (Fig. 1). The morphological diversity of PISN light curves is analogous to that of SNe observed in the local Universe, belonging to the Type II-P class (R190), to the Type II-pec class (B190), and to the Type Ib/c class (He100 and analogs), in qualitative agreement with the RSG, BSG, and WR star progenitor, and in quantitative agreement with the simulations of Kasen et al. (2011). For comparison we add the lower-energy lower-mass counterparts for each SN type (Dessart & Hillier 2010, 2011; Dessart et al. 2011), as well as our results for a delayed-detonation model of a Chandrasekhar-mass white dwarf with  $0.67 M_{\odot}$  of  $^{56}\text{Ni}$  (Dessart et al., in prep).

These PISNe reach photospheric radii of  $\sim 10^{16}$  cm, but apart from the R190 model which retains a hot photosphere for many weeks after the explosion, we find that PISN photospheres are typically cold. On the rise to peak brightness, the photospheres of models B190 and He100 heat up from  $\sim 4000$  K to  $\sim 6000$  K. Fading after peak, all PISN photospheres cool to  $\sim 4000$  K within 100-200 d. As they turn nebular, there is no longer any photosphere, nor any trapped energy, and the ejecta continue to cool, reaching typically  $\gtrsim 1000$  K three years after the explosion. So, the large initial  $^{56}\text{Ni}$  mass that causes the large peak brightness is no guarantee of high photospheric temperatures.

Spectroscopically, our PISN simulations reflect in many ways the properties of lower-mass lower-energy SNe II-P, II-pec, and Ib/c (Dessart et al. 2012). For model He100, the proposed model for SN 2007bi, our synthetic spectra become bluer on the rise to peak due to decay heating (Fig. 2). Bound-bound and bound-free processes in IMEs dominate the opacity, producing lines of Ca II, Mg I, Mg II, Si II, and O I. As the photosphere recedes deeper into the ejecta, at and beyond the peak of the light curve, the mass fraction of iron-group elements (IGEs) in the photosphere increases, and so do the effects of line blanketing, first by Fe II, and later by Fe I. Exacerbated by the photosphere cooling, the emergent spectrum reddens, fading strongly short-ward of  $5000 \text{ \AA}$ . By 500 d after explosion, the spectrum is nebular and reveals lines of O I and Ca II.

With a peak  $M_{\text{bol}} \sim -20.2$  ( $M_R = -20.5$ ) and slow nebular fading, our model He100 reproduces well the light curve morphology of SN 2007bi, although it is too faint by  $\sim 0.8$  mag in  $R$ . The red color of model He100 at 54 d after peak ( $B - R = 1.47$ )

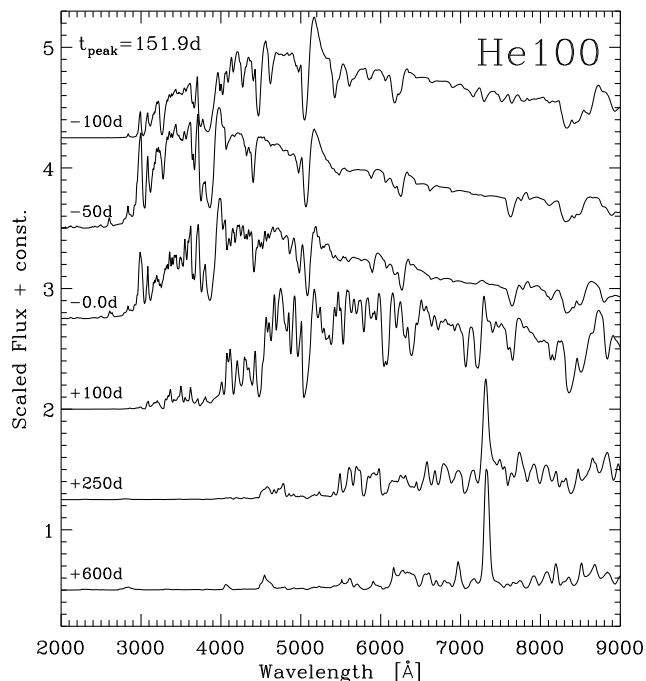


**Figure 2.** Montage of synthetic spectra for model He100. Labels on the left give the days since the bolometric maximum at 151.9 d after explosion.

strongly contrasts with the blue color of SN 2007bi at that time (we estimate  $B - R \sim 0.45$  mag from the observed spectrum while Young et al. 2010 infer a K-corrected  $B - R$  of 0.23 mag).

Further beyond the peak, model He100 shows a spectrum strongly blanketed by Fe II and Fe I, with narrow lines that form in ejecta regions moving at  $\lesssim 4000 \text{ km s}^{-1}$ , and little flux shortward of  $5000 \text{ \AA}$  (Fig. 2). This contrasts with SN 2007bi which shows a sustained blue spectrum with significant flux shortward of  $3500 \text{ \AA}$  and broad lines of Ca II, Fe II, Si II, which form in an ejecta expanding at  $\gtrsim 6000 \text{ km s}^{-1}$  (Gal-Yam et al. 2009). Model He100, proposed by Gal-Yam et al. (2009) as viable for SN 2007bi, is thus disfavored on numerous grounds. While  $^{56}\text{Ni}$  is a suitable energy source for producing a super-luminous SN, the associated IGE line blanketing and cool photospheric temperatures after the light-curve peak conspire to produce spectra that are red, rather than blue as observed in SN 2007bi, or generally in super-luminous SNe.

The apparently satisfactory spectral fit obtained by Kasen et al. (2011) results from the inadequate choice of epoch for their He100 model spectrum, as they use a 50-d pre-peak synthetic spectrum to match the 50-d post-peak spectrum of SN 2007bi. The color change as the PISN model bridges the peak was thus unfortunately ignored. Gal-Yam et al. (2009) find a match to the low-quality nebular-phase spectrum but do not model the earlier higher-quality observations nor do they explain the early blue colors, the weak blanketing, the broad features, or the apparent transition to a nebular spectrum between  $\sim 400$ - $500$  d after peak. Their estimate of a 100 B kinetic energy (ignoring the  $\sim 10$  B binding energy of the progenitor) requires a much more efficient burning than they claim, yielding not  $\sim 5 M_{\odot}$  as suggested but few  $10 M_{\odot}$  of  $^{56}\text{Ni}$  — this then places the luminosity at odds with the SN 2007bi light curve.

Proposing a consistent PISN model that matches the light curve, the color evolution, and the spectral properties (ions, line-



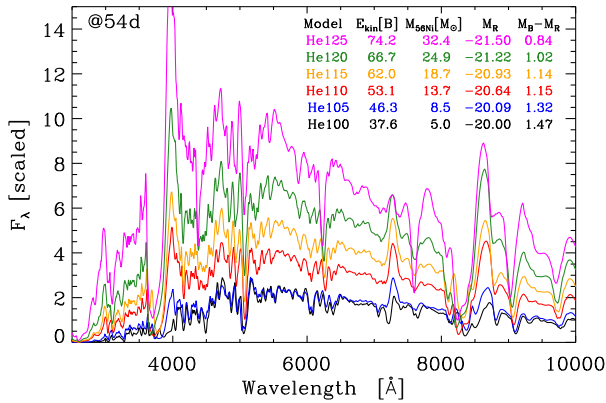


**Figure 3.** Montage of synthetic spectra for models He100 to He125 at 54 d after peak. Models of increasing  $M_{56\text{Ni}}/M_{\text{ejecta}}$  have bluer colors, although redder than SN 2007bi, whose  $B - R \sim 0.45$  at that time.

profile widths and strengths etc.) as well as agrees with massive-star evolution and formation is a considerable challenge. As a reminder, standard stellar-evolutionary models do not support the existence of Type Ic PISNe at metallicities as high as  $Z_{\odot}/3$  (Langer et al. 2007), even if suitable super-massive progenitors existed. In the next section, we discuss two different models that may cure some of the discrepancies between model He100 and SN 2007bi, and also generalize our ideas to other, non-interacting, super-luminous SNe.

#### 4 BLUE-COLORED SUPER-LUMINOUS SNe

Despite the large initial  $^{56}\text{Ni}$  mass, the large ejecta mass in model He100 renders the heating from decay ineffective at producing and sustaining a hot photosphere/ejecta. One remedy is to increase the  $^{56}\text{Ni}$  mass to ejecta mass ratio, from the 5% in model He100, quite typical of core-collapse SNe, to few tens of percent, more typical of SNe Ia. In SNe Ia, blanketing is certainly severe, but the enhanced heating produces relatively bluer colors. This in part stems from the lower mass of the ejecta, which turns transparent at  $\sim 30$  d (rather than  $\sim 300$  d), i.e., when the decay-energy rate is  $\sim 10$  times larger.

To experiment with this idea, we ran models similar to He100 but with masses between 105 and 125  $M_{\odot}$ . When exploding as PISNe, these synthesize between 8.5 and 32.4  $M_{\odot}$  of  $^{56}\text{Ni}$ . The spectra at 54 d post peak (selected to correspond to the first spectrum of 07bi) are now bluer, and the more so as the  $^{56}\text{Ni}$ -to-ejecta mass ratio increases from 8 to 26% (Fig. 3; labels give additional model properties). While models He105-He115 better match the luminosity of SN 2007bi (Fig. 1), they retain a similar, and discrepant, color as model He100. For model He125, despite obvious signs of blanketing by Fe II, the color matches more closely that of SN 2007bi, but this model is now 1 mag too bright in the  $R$ -band. In a similar fashion to model He100 and SNe Ia, it will not only be heated by 32  $M_{\odot}$  of  $^{56}\text{Ni}/^{56}\text{Co}$ , but it will also be drastically reddened by 32  $M_{\odot}$  of iron  $\gtrsim 200$  d after explosion.

What emerges, though, is the difficulty, even for extreme  $^{56}\text{Ni}$  yields, to produce high photospheric temperatures. Being fundamentally associated with large ejecta masses and huge explosion energies, PISN ejecta inevitably recombine: their photospheres adjust to reside in the transition zone between optically thick and thin conditions. Consequently, their spectra tend to peak in the optical,

reflecting the low recombination temperature of the dominant ion at the photosphere (as in SNe II-P; Dessart & Hillier 2011).

This difficulty of the PISN scenario motivated us to explore the radiative signatures that would result from delayed energy injection, as in a magnetar. Woosley (2010) studied this context in otherwise “standard” core-collapse SN explosions, although he focused exclusively on the resulting bolometric light curve. We already know that with arbitrary choices of ejecta mass, magnetic field, and initial spin, a broad diversity of luminous light curves can be produced (Kasen & Bildsten 2010). Here, we investigate the spectroscopic properties of an ejecta subject to an energy injection  $E_{\text{dep}}$  at a constant rate up to a post-explosion time  $\delta t$  (given the many parameters tuning this scenario, it is not critical for our exploration to be more accurate). We simulate this scenario with v1D using the approach of Dessart et al. (2010) starting from a 1.56 B 6.94  $M_{\odot}$  ejecta (with 0.17  $M_{\odot}$  of  $^{56}\text{Ni}$ ) produced from the explosion of an 8.74  $M_{\odot}$  WC star (model s40 of Woosley et al. 2002). Using a unique  $\delta t = 20$  d, we compute models with  $E_{\text{dep}} = 0.1, 0.3,$  and  $1.0$  B (models pm0p1, pm0p3, and pm1p0), producing 40-d broad bolometric light-curve peaks  $\sim 30$  d after explosion with representative luminosities of  $10^9$  to  $10^{10} L_{\odot}$ . Were these luminosities powered by  $^{56}\text{Ni}$  decay alone, they would require  $\gtrsim 1 M_{\odot}$  of  $^{56}\text{Ni}$ , an amount anomalously large for standard Type Ib/c SNe.

Using the v1D ejecta structure around the broad light-curve peak, we generate steady-state non-LTE spectra with CMFGEN (Fig. 4). For the lowest energy injection (model pm0p1), the heating is very weak and produces hardly any hardening of the spectrum compared to the default model with no energy injection (thus not shown). However, by increasing the deposition of energy from 0.1 B (pm0p1) to 1.0 B (pm1p0), the colors of the resulting spectrum dramatically harden. We obtain bluer spectra roughly compatible with SN 2007bi, the peculiar SN Ib 2005bf (Folatelli et al. 2006), and even the 2005ap-like event PTF09atu (Quimby et al. 2011). These three models mimic the effect of magnetars/pulsars of varying powers, something not unexpected from nature.

SNe that are super luminous due to the magnetar-energy deposition do not suffer from excess line blanketing inherent to an anomalously large production of  $^{56}\text{Ni}$ , which is inevitable in PISNe and other extreme core-collapse SN events. Instead, the extra energy injected heats the material and thermally excites the gas (provided thermalization takes place), producing lines of Si II, C II, and He I (SNe 2005bf and 2007bi; model pm0p1), and in extreme cases O II, C II, Si III, and Fe III (PTF09atu; model pm1p0). This exploration is not fully satisfactory (e.g., [Ca II] 7300 Å is not predicted in pm0p1 but is seen in SN 2007bi), but it is indicative — the spectra of these models are more fundamentally in agreement with SN 2007bi than  $^{56}\text{Ni}$ -powered super-luminous SN models. The 0.11  $M_{\odot}$  of helium in our “pm” models is thermally excited and produces He I lines. The temperatures are, however, too low, even in model pm1p0, to produce He II emission (e.g., at 4686 Å), as observed in SN 2008es (Gezari et al. 2009).

In contrast to the irrevocably high-mass PISNe, magnetar-powered ejecta, which can be of any mass, can naturally produce broad lines at all times. The large energy needed to power the light curve launches a snow-plow of the inner ejecta layers, forming a dense shell at constant velocity. This inner shell velocity is 3000  $\text{km s}^{-1}$  in model pm0p1, 3800  $\text{km s}^{-1}$  in pm0p3, and 5000  $\text{km s}^{-1}$  in pm1p0. In SN 2007bi, the width of spectral features hardly changes from 54 d until 414 d after the light-curve peak, something difficult to explain with the He100 PISN model (Fig. 2). Non-local energy deposition can counteract the recession of the spectral formation region, but this influences the most optically-

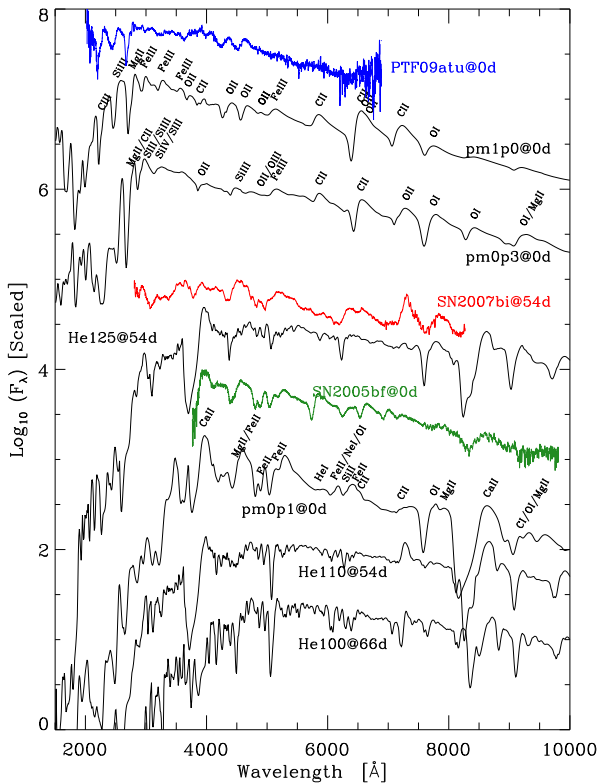


**Figure 4.** Comparison between SNe PTF09atu, 2007bi, and 2005bf, synthetic spectra of PISN models He100, He110, and He125, and magnetar-powered models pm0p1, pm0p3, and pm1p0. Some dust extinction ( $E(B - V) = 0.4$  mag) is applied to the last two models for convenience. Labels indicate the time since bolometric maximum.

thick lines and will struggle to produce broad nebular lines in such massive PISN ejecta; its impact is inhibited due to the low-metallicity of our PISN model.

An interesting issue about super-luminous SNe is their systematic detection near, or after, the peak of the light curve. In the  $^{56}\text{Ni}$ -powered model, the heat generated at depth in these massive ejecta conspires to produce a near symmetric light-curve peak (Fig. 1), and so one would expect to discover a fraction of these on the relatively long rise to peak. In the magnetar model, the lack of a pre-peak detection is naturally explained: The relatively large  $B$  and  $\Omega$  needed to power the light curve imply a fast spin down, and a fast rise to the light-curve peak is compatible with a low/moderate mass ejecta. Similarly, the post-peak fading may cover a range of slopes reflecting the differing instantaneous contributions of  $^{56}\text{Ni}$  and magnetar-energy injection.

The magnetar model is also well supported by the large number of such objects in the Galaxy (Muno et al. 2008). They are obviously easy to form, in contrast with PISNe, expected to exist primarily in the Early Universe. They are also routinely produced at low metallicity by massive-star evolution with fast rotation (Woosley & Heger 2006; Georgy et al. 2009), perhaps providing an alternate channel to black-hole formation (Dessart et al. 2008; Metzger et al. 2011; Dessart et al. 2012).

Future work requires the modeling of magnetar radiation in various massive-star progenitors using V1D and CMFGEN to characterize the range of super-luminous SNe this scenario can produce in terms of ejecta, spectral, and light-curve properties, e.g., rise time, peak luminosity, color, and fading-rate at nebular times.

## ACKNOWLEDGMENTS

LD and SB acknowledge support from European-Community grant PIRG04-GA-2008-239184 and from ANR grant 2011-Blanc-SIMI-5-6-007-01. DJH acknowledges support from STScI theory grants HST-AR-11756.01.A and HST-AR-12640.01, and NASA theory grant NNX10AC80G.

## REFERENCES

- Barkat Z., Rakavy G., Sack N., 1967, *Phys. Rev. Lett.*, 18, 379  
 Bromm V., Larson R. B., 2004, *ARA&A*, 42, 79  
 Buras R., Janka H.-T., Rampp M., Kifonidis K., 2006, *A&A*, 457, 281  
 Burrows A., Dessart L., Livne E., Ott C. D., Murphy J., 2007, *ApJ*, 664, 416  
 Colgate S. A., McKee C., 1969, *ApJ*, 157, 623  
 Dessart L., Burrows A., Livne E., Ott C. D., 2008, *ApJL*, 673, L43  
 Dessart L., Hillier D. J., 2010, *MNRAS*, 405, 2141  
 Dessart L., Hillier D. J., 2011, *MNRAS*, 410, 1739  
 Dessart L., Hillier D. J., Li C., Woosley S., 2012, *MNRAS*, 424, 2139  
 Dessart L., Hillier D. J., Livne E., Yoon S.-C., Woosley S., Waldman R., Langer N., 2011, *MNRAS*, pp 565+  
 Dessart L., Livne E., Waldman R., 2010, *MNRAS*, 408, 827  
 Dessart L., O'Connor E., Ott C. D., 2012, *ApJ*, 754, 76  
 Folatelli G., Contreras C., Phillips M. M., Woosley S. E., Blinnikov S., et al. 2006, *ApJ*, 641, 1039  
 Gal-Yam A., Mazzali P., Ofek E. O., Nugent P. E., Kulkarni S. R., Kasliwal M. M., Quimby R. M., et al. 2009, *Nature*, 462, 624  
 Georgy C., Meynet G., Walder R., Folini D., Maeder A., 2009, *A&A*, 502, 611  
 Gezari S., Halpern J. P., Grupe D., Yuan F., Quimby R., et al. 2009, *ApJ*, 690, 1313  
 Heger A., Woosley S. E., 2002, *ApJ*, 567, 532  
 Hillier D. J., Dessart L., 2012, *MNRAS*, 424, 252  
 Hillier D. J., Miller D. L., 1998, *ApJ*, 496, 407  
 Kasen D., Bildsten L., 2010, *ApJ*, 717, 245  
 Kasen D., Woosley S. E., Heger A., 2011, *ApJ*, 734, 102  
 Langer N., Norman C. A., de Koter A., Vink J. S., Cantiello M., Yoon S.-C., 2007, *A&A*, 475, L19  
 Livne E., 1993, *ApJ*, 412, 634  
 Maeda K., Tanaka M., Nomoto K., Tominaga N., Kawabata K., et al. 2007, *ApJ*, 666, 1069  
 Metzger B. D., Giannios D., Thompson T. A., Bucciantini N., Quataert E., 2011, *MNRAS*, 413, 2031  
 Moriya T., Tominaga N., Tanaka M., Maeda K., Nomoto K., 2010, *ApJL*, 717, L83  
 Muno M. P., Gaensler B. M., Nechita A., Miller J. M., Slane P. O., 2008, *ApJ*, 680, 639  
 Paxton B., Bildsten L., Dotter A., Herwig F., Lesaffre P., Timmes F., 2011, *ApJS*, 192, 3  
 Quimby R. M., Kulkarni S. R., Kasliwal M. M., Gal-Yam A., Arcavi I., et al. 2011, *Nature*, 474, 487  
 Scannapieco E., Madau P., Woosley S., Heger A., Ferrara A., 2005, *ApJ*, 633, 1031  
 Smith N., Li W., Foley R. J., Wheeler J. C., et al. 2007, *ApJ*, 666, 1116  
 Waldman R., 2008, *ApJ*, 685, 1103  
 Wheeler J. C., Yi I., Höflich P., Wang L., 2000, *ApJ*, 537, 810  
 Woosley S. E., 2010, *ApJL*, 719, L204

Woosley S. E., Heger A., 2006, *Astrophys. J.*, 637, 914

Woosley S. E., Heger A., Weaver T. A., 2002, *Reviews of Modern Physics*, 74, 1015

Young D. R., Smartt S. J., Valenti S., Pastorello A., Benetti S.,  
Benn C. R., Bersier D., et al. 2010, *A&A*, 512, A70